Geological and Atmospheric Sciences Publications   Geological and Atmospheric Sciences

4-2004

A conceptual and scaling evaluation of the surface wetness effect on daytime moisture convergence along a surface cold front with differential cloud cover

Moti Segal
Iowa State University, segal@iastate.edu

Eric Anthony Aligo
Iowa State University, ealigo@gmail.com

William A. Gallus Jr.
Iowa State University, wgallus@iastate.edu

A conceptual and scaling evaluation of the surface wetness effect on daytime moisture convergence along a surface cold front with differential cloud cover

Abstract

A conceptual evaluation and scaling of the potential impact of surface wetness on spring/summer midlatitude daytime surface cold front moisture convergence is presented. First, a simplified expression is derived, evaluating the effect of surface wetness on frontal moisture convergence due to a differential cloud-cover-induced thermal gradient perturbation. It indicates that wet surfaces may be conducive to enhanced moisture convergence compared with dry surfaces only for very high values of both the cross-frontal relative wind component and the frontal background vertical velocity. With increased background specific humidity in the warm sector, decreased cross-frontal relative wind speed, and a less stable early morning temperature lapse rate, dry surface conditions are significantly more conducive to enhanced frontal moisture convergence. When the daytime boundary layer thermal destabilization effects on the frontal updraft are considered, generally insignificant modifications of the above patterns of frontal moisture convergence are indicated. Overall, the evaluation suggests that typically dry surfaces better promote daytime frontal moisture convergence than wet surfaces, a result that is counterintuitive.

NOTES AND CORRESPONDENCE

A Conceptual and Scaling Evaluation of the Surface Wetness Effect on Daytime Moisture Convergence along a Surface Cold Front with Differential Cloud Cover

MOTI SEGAL

Agricultural Meteorology Program, Department of Agronomy, Iowa State University, Ames, Iowa

ERIC A. ALIGO AND WILLIAM A. GALLUS JR.

Department of Geological and Atmospheric Sciences, Iowa State University, Ames, Iowa

ABSTRACT

A conceptual evaluation and scaling of the potential impact of surface wetness on spring/summer midlatitude daytime surface cold front moisture convergence is presented. First, a simplified expression is derived, evaluating the effect of surface wetness on frontal moisture convergence due to a differential cloud-cover-induced thermal gradient perturbation. It indicates that wet surfaces may be conducive to enhanced moisture convergence compared with dry surfaces only for very high values of both the cross-frontal relative wind component and the frontal background vertical velocity. With increased background specific humidity in the warm sector, decreased cross-frontal relative wind speed, and a less stable early morning temperature lapse rate, dry surface conditions are significantly more conducive to enhanced frontal moisture convergence. When the daytime boundary layer thermal destabilization effects on the frontal updraft are considered, generally insignificant modifications of the above patterns of frontal moisture convergence are indicated. Overall, the evaluation suggests that typically dry surfaces better promote daytime frontal moisture convergence than wet surfaces, a result that is counterintuitive.

1. Introduction

Numerical model and observational studies have indicated a noticeable daytime increase in the cross-frontal temperature gradient resulting in an enhanced cross-frontal circulation for cold fronts possessing a cloud-covered cold sector and cloudless warm sector with a relatively dry surface (e.g., Segal et al. 1993; Koch et al. 1995; Miller et al. 1996; Gallus and Segal 1999; Sanders 1999, among others). The impact of surface wetness on such cold front moisture-related processes is an additional issue of special interest. Increased surface wetness only secondarily affects the daytime frontal temperature gradient, the convective boundary layer (CBL) depth and turbulence, and thus the related dynamical contributions to frontal convergence (Segal et al. 1993). However, the increased surface wetness enhances frontal moisture convergence by increasing moisture in the warm sector. The interplay between the surface wetness level and its impact on frontal moist

processes is thus an intriguing issue that has motivated this note.

Observations of cold front activity occasionally imply the potential significance of the surface wetness effect on frontal moisture convergence. For example, some observed intense surface cold fronts lack significant precipitation when relatively dry lower atmospheric conditions exist. Likewise, observed weak cold fronts, though associated with a humid atmosphere, occasionally lack noticeable precipitation because of weak frontal flow convergence. Koch et al. (1997) found that a reduction of surface wetness in a simulated spring cold front was conducive somewhat to a corresponding intensification of the front's dynamical effects. Gallus and Segal (1999) found similar effects in response to changes in surface wetness for a late winter cold front. An indirect observational indication on the potential impact of surface wetness on frontal convection can be inferred, for example, from the studies of Rabin et al. (1990) and Curtim et al. (1995). Additional numerical model sensitivity tests would be needed in order to evaluate more definitively the interrelationship between surface wetness and surface cold front potential rainfall activity. However, a generalization of this interrelationship based

Corresponding author address: Moti Segal, Agricultural Meteorology, Dept. of Agronomy, Iowa State University, 3010 Agronomy Hall, Ames, IA 50011.
E-mail: segal@iastate.edu

on conceptual evaluations and a simplified scaling accounting for the main forcing of frontal moisture convergence would be useful and is thus presented. Although such an approach provides only a bulk estimation while being confined to simplified situations, it may reveal certain frontal moisture convergence patterns and their sensitivity to surface wetness. Additionally, it may guide the construction of numerical model sensitivity simulations.

2. Scaling

a. Basic parameters

1) MOISTURE CONVERGENCE

In the following, a simple scaling is provided while considering the afternoon hours in which the accumulated daily thermal/evapotranspiration effect should be near its peak. Assuming a 2D surface cold front, we explore the surface wetness conditions in which the vertically integrated horizontal moisture convergence at the edge of the front, con $= -\int_0^H \partial(uq^*)/\partial x\, dz$, is maximized ($u$ here is the cross-front velocity component at the front, q^* is the specific humidity, and H is a characteristic height scale). The characteristic height scale is defined in our study as the maximum depth of the lower atmosphere that can be affected by the daytime surface thermal forcing and acquires relatively high q^* values. Therefore, in the presented scaling the depth of this layer is assumed to be equivalent to that of a CBL over a dry surface (commonly the specific humidity decreases noticeably above the CBL top). Typically, for surface cold fronts, the convergence zone is located in the warm sector near the leading edge of the front, thus q^* in the nearby warm sector will be considered. Considering a horizontally uniform distribution of q^* in the warm sector of the front and denoting q as the vertically averaged q^* within the layer considered for moisture convergence, then for scaling purposes con $\sim -\int_0^H q(\partial u/\partial x)\, dz$, or using the continuity equation, con $\sim [wq]$ (where w is the scaled upward vertical velocity associated with the frontal convergence; the details of the scaling of w are presented later). Analogous to Alpert (1986), the value of $[wq]$ indicates the potential frontal rainfall activity. It can be assumed that maximizing $[wq]$ at the frontal convergence zone potentially would increase the related rainfall.

A schematic illustration pertinent to the scaling is presented in Fig. 1. We assume a steady-state surface cold front in the early morning hours with a cloudy cold sector and a clear warm sector. Starting from this stage, the response of the frontal moisture convergence in the afternoon hours to changes in a prescribed surface wetness level throughout the area affected by the front will be evaluated using a perturbation approach. It can be reasonably assumed that the daytime surface sensible and latent heat fluxes in the cold sector are negligibly small because of the cloud shading effect. In the warm
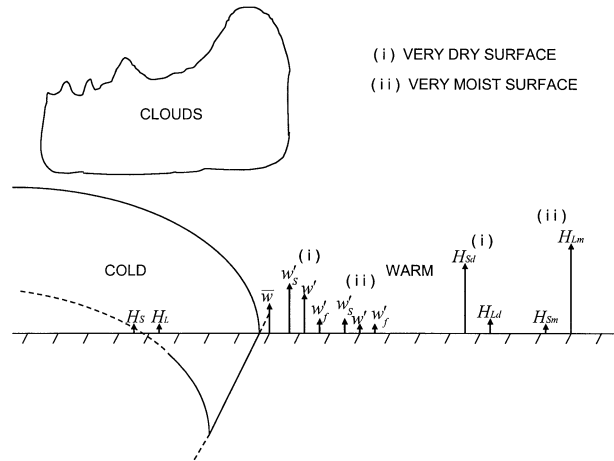

FIG. 1. Schematic illustration of the cold front situation evaluated in the scaling. Variable definitions are provided in the text. The sensible and latent heat fluxes are depicted by arrows indicating their relative magnitudes (the subscripts d and m indicate very dry and very moist surfaces, respectively).

sector, a clear sky is assumed to be maintained. Thus the sensible and latent heat flux values there are directly related to the wetness of the surface. Cloud diabatic effects of condensation and evaporation processes are not considered. Separating the scaled variables into background values, $\overline{(\ )}$ (reflecting the front's early morning conditions), and of the perturbations related to the effects of daytime surface wetness changes, $(')$, yields

$$[wq] = (\overline{w} + w' + w'_s + w'_f)(\overline{q} + q')$$
$$= \overline{w}\,\overline{q} + \overline{w}q' + (w' + w'_s + w'_f)\overline{q}$$
$$+ (w' + w'_s + w'_f)q', \qquad (1)$$

where the last three terms on the rhs of (1) are associated with the daytime changes in the frontal vertical velocity and specific humidity. Here w' denotes the vertical velocity perturbation induced by the daytime modification of the cross-frontal thermal gradient forced by the differential sensible heat flux across the front. The variable w'_s reflects the daytime intensification of the frontal updraft due to thermal destabilization of the lower atmosphere by sensible heat (see, e.g., Koch et al. 1995). The vertical velocity, w'_f, is due to the modification of the geostrophic alongfront flow in the warm sector of the front by daytime CBL turbulence that leads to the formation of a cross-frontal wind component (in the cold sector, cloud shading prevents an enhancement of the daytime turbulence). Following Koch et al. (1995), w'_s is several times larger than w'_f; thus, for simplification and as a first approximation, we neglected frictional effects in the presented scaling. It is assumed that the location of the upward velocity cells contributing to w' and w'_s overlap that of $\overline{w}$ (the impact of a deviation from this assumption will also be considered). The daytime

change in specific humidity within the moisture convergence layer of depth H is denoted as q'.

2) THERMAL-GRADIENT-PERTURBATION-INDUCED VERTICAL VELOCITY

In the scaling, the vertical velocity perturbation, w', is analogous to that generated by a sea-breeze circulation. The induced thermal circulation perturbation develops in the warm sector of the front and together with its forcing (the cold sector cloud cover) is advected at the frontal system speed, c (e.g., Segal et al. 1993). The following scaling relation was adopted to estimate the magnitude of w' (Mahrt et al. 1994, p. 2489):

$$w' = \frac{1}{U_r^2}\left(\frac{H_S}{\rho c_p T_o}\right)gh. \tag{2}$$

Denoting U as the background cross-frontal component of the mean flow in the warm sector, then $U_r = U - c$ is the corresponding scaled cross-frontal flow component relative to the front. Here H_S is the characteristic surface sensible heat flux in the warm sector of the front during the period τ (from morning to afternoon); ρ ($\sim$1.2 kg m^{-3}) and T_o ($\sim$300 K) are the characteristic background air density and temperature, respectively, within the depth h (depth of the CBL in the warm sector); and c_p and g follow conventional notation. Considering an analogy to a sea breeze, when $c > U$, U_r is equivalent to an offshore background flow relative to the induced thermal circulation. In the derivation of (2) it is assumed that $|U_r| > 0$; when $|U_r| \sim 0$ a modified version of (2) should be adopted (see Mahrt et al. 1994).

The depth of the frontal warm sector CBL is approximated as (e.g., Tennekes 1973)

$$h = \left(\frac{2c_e \int_o^\tau H_S \, dt}{\rho c_p \beta_o}\right)^{1/2}, \tag{3}$$

where β_o is the characteristic morning potential temperature lapse rate in the layer above the CBL, and c_e ($\sim$1.2) is an entrainment coefficient at the top of the CBL.

In Mahrt et al. (1994) the friction and the Coriolis force are not considered in the scaling of the generated perturbed thermal circulation. As with a sea breeze, these two forces reduce the cross-frontal component of this circulation (through frictional losses and flow veering) and therefore the related contribution to w' (e.g., Atkinson 1981). Thus, conceptually, w' represents the maximum possible vertical velocity forced by the cross-frontal gradient in H_S. On the other hand, the linear approach associated with the scaling (because of the use of domain averaged variables) tends to underestimate the intensity of the real world w'. A comparison of the scaled w' values, based on (2), with corresponding nu-

merical-model-simulated values for sea breezes reported in Arritt (1993) indicated a reasonable agreement.

It is difficult to directly scale the value of w'_s. Following the various evaluations in Koch et al. (1995), it is assumed in a bulk estimation that $w'_s \geq w'$. Since a reliable scaling of w' is obtained by applying (2), using the value of w' as a reference enables the consideration of the w'_s contribution to the frontal moisture convergence.

3) LOWER-ATMOSPHERE MOISTURE PERTURBATION

Expressing the surface wetness through the Bowen ratio, B ($=H_S/H_L$) (where H_L is the characteristic surface latent heat flux), then q' is estimated based on the contribution of latent heat flux to the specific humidity within the considered moisture convergence layer during the period τ:

$$q' = \frac{\tau B^{-1} H_S}{\rho H \lambda}, \tag{4}$$

where λ is the latent heat of vaporization.

4) EVALUATED SURFACE WETNESS SITUATIONS AND RELATED ASSUMPTIONS

As a first approximation, $H_S + H_L \sim constant$ for varying surface wetness situations (i.e., the surface moist enthalpy flux components are merely repartitioned in response to changes in the surface wetness), and also, following (3), $h \propto H_S^{1/2}$. Under these constraints, substituting (2), (4), and an estimated w'_s into (1) yields an equation for the dependence of $[wq]$ on B and the meteorological background variables. In practice, however, solving such an equation for a continuous range of B values would result in a complex expression for $[wq]$, while requiring additional closure assumptions. It would be therefore more beneficial to focus on extreme dry and moist surface wetness situations as they can be contrasted using simplified derived expressions. These two situations are the most interesting when investigating the surface wetness effect on moisture convergence. An estimation of this effect for intermediate values of B can be obtained, in a first approximation, by interpolating linearly between those two extreme surface wetness conditions. Adopting this approach, we examine the perturbation in $[wq]$ obtained for the following situations: (i) a very dry surface [$B^{-1} \sim 0$; thus, $H_L \sim 0$, and $H_S \sim (R_N - G)_d$, where R_N is the net radiation and G the subsurface thermal flux], and (ii) a very moist surface [$B^{-1} \gg 1$; thus, $H_L \sim (R_N - G)_m$]. The subscripts d and m indicate very dry and very moist surface conditions, respectively. In the following several scaling assumptions are outlined, while their detailed justification is found in the appendix. Based on (i) it can be assumed that for scaling purposes $q'_d \sim 0$ as the daytime contribution of evapotranspiration to the CBL in the warm sector of the front, under very dry surfaces, is

negligible. Also, $w'_m \sim 0$ as the daytime H_S values within the warm sector of the front, under very moist surfaces, are very small, whereas in the cloudy cold sector H_S values can be assumed to be very low because of reduced solar irradiance reaching the surface. For the vertical velocity, w'_{sm}, generated by the daytime destabilization associated with the development of the CBL over a very moist surface, it is assumed that $w'_{sm} \sim w'_{sd}/3$.

b. Scaling of surface wetness impact on frontal moisture convergence under an ideal assumption

Ideally prescribed $w'_{sm} \sim 0$ is assumed here to derive simplified scaling expressions. These expressions will be used later in the ideal evaluations in section 3a, as well as scaling parameters for the evaluation under the nonideal condition in section 3b. Considering the constraints stated above and using (1), while omitting w'_f following the elaboration given in section 2a(1), we derive the daytime departure of the frontal moisture convergence from its early morning value, denoted henceforth by Δ. For the very dry surface case, substituting w'_d based on (2) and $q'_d \sim 0$ into (1) yields

$$\Delta_d = ([wq]_d - \overline{w}\,\overline{q}) = \frac{1}{U_r^2}\left(\frac{H_{Sd}}{\rho c_p T_o}\right)gh_d\overline{q} + w'_{sd}\cdot\overline{q}, \quad (5)$$

where H_{Sd} is the characteristic sensible heat flux for the very dry surface case in the warm sector of the front during the period τ. For the very moist surface case, substituting q' based on (4) (with $H = h_d$; following the definition of H in section 1), $w'_m \sim 0$, and ideally prescribed $w'_{sm} \sim 0$ into (1) yields

$$\Delta_m = ([wq]_m - \overline{w}\,\overline{q}) = \overline{w}\left(\frac{\tau H_{Lm}}{\rho h_d \lambda}\right), \quad (6)$$

where H_{Lm} is the corresponding characteristic latent heat flux for the very moist surface case.

For a given $(\overline{w}\,\overline{q})$, the ratio $\varepsilon_I = \Delta_d/\Delta_m$ implies the surface wetness impact on frontal moisture convergence under the ideal assumption stated above. Values of $\varepsilon_I > 1$ indicate that the very dry surface case is more supportive for frontal moisture convergence than the very moist surface case, whereas $\varepsilon_I < 1$ indicates the reverse. The variable ε_I can be presented as

$$\varepsilon_I = \varepsilon_o + \varepsilon_s, \quad (7)$$

where ε_o provides a measure for the relative sensitivity of frontal daytime moisture convergence to surface wetness conditions due to the horizontal thermal gradient perturbation. The value of ε_s provides an estimate of the relative contribution to the moisture convergence because of daytime thermal destabilization of the lower atmosphere by sensible heat flux.

Considering a nonlinear interaction of the processes associated with the formation of w' and w'_s, it may be suggested in a conservative consideration to replace ε_I, given by (7), with ε_I^*, defined as

$$\varepsilon_I^* = \max(\varepsilon_o, \varepsilon_s). \quad (8)$$

The value of ε_o is the ratio of the first term on the rhs of (5) to the rhs term of (6) and is given as

$$\varepsilon_o = \frac{gh_d^2\lambda\overline{q}}{\tau c_p \overline{w} U_r^2 T_o}\cdot\frac{H_{Sd}}{H_{Lm}}. \quad (9)$$

The value of ε_s is the ratio of the second term on the rhs of (5) to the rhs term of (6). Following section 2a(2) $w'_{sd} \geq w'_d$; therefore, the relation $\varepsilon_s \geq \varepsilon_o$ is applicable.

3. Evaluation of the surface wetness impact on frontal moisture convergence

a. Evaluation under an ideal wet surface assumption

In the following we estimate the possible range of values for ε_o and ε_s, which implies the magnitude of ε_I and ε_I^*. Initially, the frontal thermal gradient perturbation effect is evaluated, then the potential additional contribution of daytime destabilization within the CBL is estimated. Since it is assumed here ideally that $w'_{sm} \sim 0$, the evaluation of ε_I and ε_I^* will provide an upper limit to the surface wetness impact on frontal moisture convergence. Additionally, however, the results obtained here will be used in section 3b in the evaluation of the general case in which the ideal wet surface assumption is removed.

The expression for ε_o in (9) can be further simplified. For scaling purposes, to a first approximation, $H_{LM} \sim H_{Sd}$. However, based on surface thermal flux characteristics it can be shown that H_{Lm} would be somewhat larger than H_{Sd}, by as much as 25% (e.g., Fig. 5 of Segal et al. 1988; Fig. 4 of Segal et al. 1995); thus, in a conservative consideration $H_{Lm} \approx 1.25\,H_{Sd}$ is adopted. Substituting numerical values for the constants in (9), in SI units, (assuming $\tau = 3 \cdot 10^4$ s, i.e., midafternoon) yields

$$\varepsilon_o = 2.17 \times 10^{-3}\,\frac{h_d^2\overline{q}}{\overline{w}U_r^2}. \quad (10)$$

Equation (10) indicates that ε_o would increase with $\overline{q}$, as a dry surface would support increased w'_d, and thus the upward transport of $\overline{q}$. Likewise, an increased value of h_d associated with a dry surface reflecting increased H_S in the warm sector would increase w'_d and the upward transport of $\overline{q}$. As $|U_r|$ increases, the value of w'_d decreases in analogy to the retarding effect of increased background flow on upward induced vertical velocities in the case of sea breezes (e.g., Arritt 1993); thus, ε_o should decrease. As the value of $\overline{w}$ increases, the significance of the contribution of w'_d to upward moisture transport decreases, resulting in again a decrease in the ε_o value. Additionally, since $h_d \propto \beta_0^{-0.5}$ based on (3), a less stable morning thermal stratification would further support enhanced frontal moisture convergence with a dry surface.

Using (10), ε_o was computed for typical ranges of $|U_r|$ ($\sim$0 to 10 m s^{-1}) and $\overline{w}$ (0.05 to 0.3 m s^{-1}; the

upper range of $\overline{w}$ is assumed to be supported by the dynamics of frontal cloud systems that might be associated with surface cold fronts). Figure 2 presents the related values of ε_o for a reference case with $\overline{q} = 0.01$ kg kg^{-1} and $h_d = 1000$ m (these are suggested as representative values for spring cold front situations). For $|U_r| < 5$ m s^{-1}, (10) yields $\varepsilon_o \gg 1$ (except for combinations of high values of $\overline{w}$), and these cases are not presented. For most other combinations of $|U_r|$ and $\overline{w}$, typically $\varepsilon_o > 1$. In a second situation we considered $\overline{q} = 0.015$ kg kg^{-1} and $h_d = 2000$ m, which may reflect a midlatitude summer situation. For this situation, following (10), ε_o is obtained by factoring the contour values in Fig. 2 by 6. It is evident that even for relatively high $|U_r|$ speed situations combined with high $\overline{w}$ values, dry surfaces are more conducive to enhanced vertical transport of moisture at the frontal interface compared with wet surface situations. One may use Fig. 2 to evaluate ε_o for any other combination of $\overline{q}$ and h_d by multiplying the contour levels by $h_d^2 \cdot \overline{q}/10^4$.

Following section 2b, $\varepsilon_s \geq \varepsilon_o$. Assuming that $\varepsilon_s = \varepsilon_o$, then using (7) and (8), respectively, $\varepsilon_I = 2\varepsilon_o$ and $\varepsilon_I^* = \varepsilon_o$. When $\varepsilon_s > \varepsilon_o$, as more likely will be the case, the values of ε_I and ε_I^* increase furthermore. Thus, under an ideal wet surface assumption and following Fig. 2, very dry surfaces are typically more conducive to enhancement of frontal moisture convergence than very moist surfaces.

b. Evaluation under a nonideal condition

In the frontal moisture convergence evaluation in section 3a we assumed ideally that $w_{sm}' \sim 0$. In the present derivation we replace this ideal assumption, following the estimation in the appendix, with $w_{sm}' \sim w_{sd}'/3$. The ratio of the frontal moisture convergence perturbation between the very dry surface and the very moist surface is estimated using the expressions ε_o and ε_s evaluated in section 3a under the ideal wet surface assumption. For the nonideal case, analogous to ε_I given by (7), using (1) [while omitting w_f' based on the elaboration given in section 2a(1)], we evaluate first $\varepsilon_{NI} = \Delta_d/\Delta_m$ [where Δ_d is given by (5) and Δ_m is based on the nonideal version of (6)] as

$$\varepsilon_{NI} = \frac{w_d'\overline{q} + w_{sd}'\overline{q}}{[\overline{w}q_m' + w_{sd}'(\overline{q} + q_m')/3]}. \quad (11)$$

Defining $r = q_m'/\overline{q}$ (where observationally, $r \leq 0.5$ is likely), then substituting $(\overline{q} + q_m') = \overline{q}(1 + r)$ in (11) and normalizing the numerator and the denominator on the rhs of (11) by $(\overline{w}q_m')$ yields

$$\varepsilon_{NI} = \frac{3\varepsilon_o + 3\varepsilon_s}{[3 + (1 + r)\varepsilon_s]}. \quad (12)$$

Following (12), $\varepsilon_{NI} > 1$ when $3\varepsilon_o + (2 - r)\varepsilon_s > 3$. Using the conservative assumption $\varepsilon_s = \varepsilon_o$ and $r = 0.5$, it can be suggested that $\varepsilon_{NI} > 1$ for all $\varepsilon_o > 0.67$, where
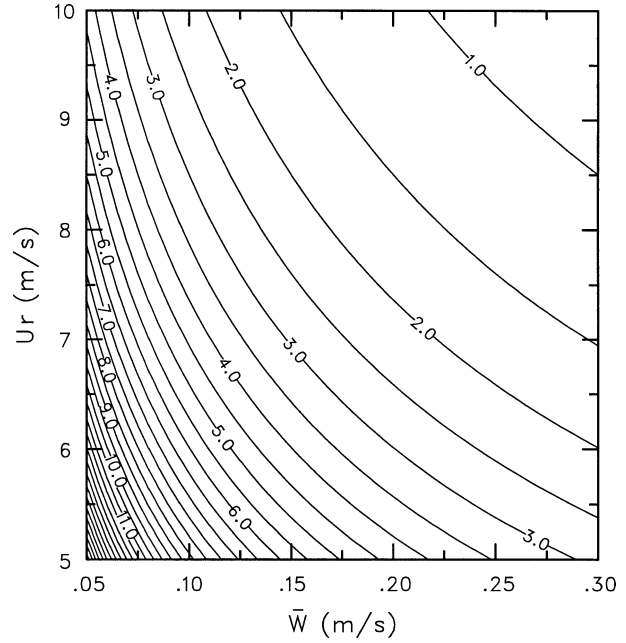

Fig. 2. Computed ε_o values [based on (10)] for various combinations of $\overline{w}$ and $|U_r|$ for $h_d = 1000$ m and $\overline{q} = 0.01$ kg kg^{-1}. Note that evaluating ε_o for any other combination of $\overline{q}$ and h_d can be obtained by multiplying the contour levels by $h_d^2(\overline{q}/10^4)$.

ε_o is given by (10) and is illustrated in Fig. 2. For $\varepsilon_s > \varepsilon_o$, $\varepsilon_{NI} > 1$ is obtained for a threshold lower than 0.67 for ε_o values.

Considering the nonlinear interaction between the updraft cells associated with w_d' and w_{sd}', it may be suggested, in a conservative consideration and analogous to (8), to replace ε_{NI} given by (12) with ε_{NI}^* defined as

$$\varepsilon_{NI}^* = \frac{\max(w_d', w_{sd}')\overline{q}}{[\overline{w}q_m' + w_{sd}'(\overline{q} + q_m')/3]}. \quad (13)$$

When the locations of the updraft cells of w_d' and w_{sd}' are not overlapping, (13) is also a reasonable approximation in an evaluation when considering the strongest updraft cell.

To evaluate ε_{NI}^* based on (13), two possible ratios have to be computed. However, following the elaboration in section 2a(2) it is likely that the w_{sd}' term in the numerator will be associated with the maximum value in (13). Therefore,

$$\varepsilon_{NI}^* = \frac{w_{sd}'\overline{q}}{[\overline{w}q_m' + w_{sd}'(\overline{q} + q_m')/3]}. \quad (14)$$

Normalizing the numerator and the denominator on the rhs of (14) by $\overline{w}q_m'$ yields

$$\varepsilon_{NI}^* = \frac{\varepsilon_s}{[1 + (1 + r)\varepsilon_s/3]}. \quad (15)$$

Thus, when $r = 0.5$, $\varepsilon_{NI}^* > 1$ for $\varepsilon_s > 2$. Specifically, considering the constraint $\varepsilon_s \geq \varepsilon_o$ then (i) when $\varepsilon_s =$

ε_o, $\varepsilon_{NI}^* > 1$ for $\varepsilon_o > 2$, and (ii) when $\varepsilon_s > \varepsilon_o$, $\varepsilon_{NI}^* > 1$ is obtained for a threshold lower than 2 for ε_o values.

Considering the results obtained with (12) or (15) and the characteristic of ε_o based on Fig. 2, it is suggested that under the nonideal condition, typically very dry surfaces better promote frontal convergence than very moist surfaces.

4. Conclusions

In this note simplified expressions were derived, using a perturbation approach, to scale the influence of extreme surface wetness conditions (very dry versus very moist) on potential afternoon moisture convergence associated with surface cold fronts. A surface cold front situation was considered with a cloudy cold sector (where the surface sensible and latent heat fluxes were assumed to be negligible) and a cloudless warm sector. The daytime frontal thermal gradient perturbation and thermal destabilization by sensible heat flux effects were estimated for their contribution to frontal moisture convergence. The sensitivity to the surface wetness of the frontal moisture convergence induced by the thermal gradient perturbation was examined through the background cross-frontal wind relative to the front, vertical velocity, specific humidity, and the CBL depth ($|U_r|$, $\overline{w}$, $\overline{q}$, and h_d, respectively) in the afternoon hours. A decrease in the value of the first two variables and an increase in the two last variables tend to enhance the cold front moisture convergence when dry surface conditions exist compared with wet surface conditions. When accounting for boundary layer thermal destabilization under an ideal wet surface assumption, frontal moisture convergence tends to be enhanced furthermore in the dry surface case. Using expressions derived in the scaling under the ideal wet surface assumption, an evaluation was carried out for a nonideal condition. Only a somewhat modified response of the frontal moisture convergence to the surface wetness was found. Overall, a somewhat counterintuitive conclusion is obtained: in most common situations, the surface moisture convergence is enhanced under dry surface conditions.

Although results were presented for two extreme surface conditions, it is suggested that intermediate patterns of moisture convergence (with nonlinear variations between these two extremes) will be found when considering moderate surface wetness conditions. As an additional point, on many occasions satellite/radar imagery indicate onset/intensification of frontal cloud lines in the afternoon hours. The dry and wet surface forcing results in a peak contribution to frontal moisture convergence in the late afternoon hours. However, forcing from the dry surface fades away following sunset because of cooling and thermal stabilization of the lower atmosphere (the formation of daytime cloudiness in the warm sector would have a similar effect). Wet surfaces maintain their daytime generated contribution (i.e., increased boundary layer moisture) also during nighttime.

Finally, evaluating the conclusion in the present study by numerical model simulations should be considered as a follow-up study.

APPENDIX

Justification of Some of the Assumptions

In the presented scaling we assumed that $q_d' \sim 0$ for the very dry surfaces, $w_m' \sim 0$, and $w_{sm}' \sim w_{sd}'/3$ for the very moist surfaces. Within the framework of scaling in this note it means that q_d' and w_m' can be neglected while resulting in a relatively small effect on the results [i.e., $q_d' \sim 0^{-1}(q_m')$ and $w_m' \sim 0^{-1}(w_d')$]. In the following we provide justification for these assumptions:

1) *Justifying the assumption, $q_d' \sim 0$.* Following (4), $q' \propto H_L$. A reasonable scaling for the ratio of H_L over a very moist surface to that over a very dry surface is $H_{Ld}/H_{Lm} \sim 0.1$ (e.g., Fig. 6 of Segal et al. 1988; Fig. 4 of Segal et al. 1995). Thus, $q_d'/q_m' \sim 0.1$; therefore q_d' can be ignored in the presented scaling.

2) *Justifying the assumption, $w_m' \sim 0$.* Following (2), $w' \propto H_S \cdot h$. Based on the studies cited in (i), $H_{Sm}/H_{Sd} \sim 0.1$, and correspondingly following (3), $h_d/h_m \sim 3$. Therefore, $w_m'/w_d' < 0.1$. The decline of w' to negligible values when the warmer section of mesoscale circulations (forced by differential sensible heat fluxes) becomes very wet can be inferred also from numerical model simulation results (see, e.g., Figs. 5 and 6 of Segal et al. 1988).

3) *Justifying the assumption, $w_{sm}' \sim w_{sd}'/3$, where w_s' is generated by the daytime thermal destabilization of the lower atmosphere by sensible heat flux. In a first approximation, w_s' is related to the depth of the CBL, in which the daytime destabilization occurs. Thus in a crude estimation, $w_s' \propto h$. Considering $h_d/h_m \sim 3$, as indicated above, then $w_{sm}' \sim w_{sd}'/3$.

REFERENCES

Alpert, P., 1986: Mesoscale indexing of the distribution of orographic precipitation over high mountains. *J. Climate Appl. Meteor.,* **25,** 532–545.

Arritt, R. W., 1993: Effects of large-scale flow on characteristic features of sea breeze. *J. Appl. Meteor.,* **32,** 116–125.

Atkinson, B. W., 1981: *Meso-scale Atmospheric Circulations.* Academic Press, 495 pp.

Cutrim, E., D. W. Martin, and R. Rabin, 1995: Enhancement of cu-

mulus clouds over deforested lands in Amazonia. *Bull. Amer. Meteor. Soc.,* **76,** 1801–1805.

Gallus, W. A., Jr., and M. Segal, 1999: Diabatic effects on late winter cold front evolution: Conceptual and numerical model evaluations. *Mon. Wea. Rev.,* **127,** 1518–1537.

Koch, S. E. J., T. McQueen, and V. M. Karyampudi, 1995: A numerical study of the effects of differential cloud cover on cold frontal structure and dynamics. *J. Atmos. Sci.,* **52,** 937–964.

——, A. Aksakal, and J. T. McQueen, 1997: The influence of mesoscale humidity and evapotranspiration fields on a model forecast of a cold-frontal squall line. *Mon. Wea. Rev.,* **125,** 384–409.

Mahrt, L., J. Sun, D. Vickers, J. I. MacPherson, J. R. Pederson, and R. L. Desjardins, 1994: Observations of fluxes and inland breezes over a heterogeneous surface. *J. Atmos. Sci.,* **51,** 2484–2499.

Miller, L. J., M. A. Lemone, W. Blumen, R. L. Grossman, M. Gamage, and R. Zamora, 1996: The low-level structure and evolution of a dry arctic front over the central United States. Part I: Mesoscale observations. *Mon. Wea. Rev.,* **124,** 1648–1675.

Rabin, R. M., P. J. Stadler, P. Wetzel, D. J. Stensrud, and M. Gregory, 1990: Observed effects of landscape variability on convective clouds. *Bull. Amer. Meteor. Soc.,* **71,** 272–280.

Sanders, F., 1999: A short-lived cold front in the southwestern United States. *Mon. Wea. Rev.,* **127,** 2395–2403.

Segal, M., R. Avissar, M. McCumber, and R. A. Pielke, 1988: Evaluation of vegetation cover effects on the generation and modification of mesoscale circulations. *J. Atmos. Sci.,* **45,** 2268–2292.

——, W. L. Physick, J. E. Heim, and R. W. Arritt, 1993: The enhancement of cold front temperature contrast by differential cloud cover. *Mon. Wea. Rev.,* **121,** 867–873.

——, R. W. Arritt, C. Clark, R. Rabin, and J. Brown, 1995: Scaling evaluation of the effect of surface characteristics on potential for deep convection over uniform terrain. *Mon. Wea. Rev.,* **123,** 383–400.

Tennekes, H., 1973: A model for the dynamics of the inversion above a convective boundary layer. *J. Atmos. Sci.,* **30,** 558–567.